Numerical studies on shear connectors in push-out tests under elevated temperatures

Aaron J. Wang*

Corporate Technical Management, CapitaLand Management (China) Co. Ltd., Shanghai, P.R. China

Abstract. Three-dimensional thermal and mechanical coupled finite element models are proposed to study the structural behaviours of shear connectors under fire. Concrete slabs, steel beams and shear connectors are modelled with eight-noded solid elements, and profiled steel deckings are modelled with eight-noded shell elements. Thermal, mechanical and geometrical nonlinearities are incorporated into the models. With the proper incorporation of thermal and mechanical contacts among steel beams, shear connectors, steel deckings and concrete slabs, both of the models are verified to be accurate after the validation against a series of push-out tests in the room temperature or under the standard fire. Various thermal and mechanical responses are also extracted and observed in details from the results of the numerical analyses, which gives a better understanding of the structural behavior of shear connectors under elevated temperatures.

Keywords: shear connector; structural fire engineering; finite element modelling; thermal analysis

1. Introduction

The structural system of a composite beam is essentially a T beam with a thin wide concrete flange connected with a steel section. The concrete flange is in compression and the steel section is largely in tension. The forces between the two materials are transferred by shear connectors, usually headed studs or other connectors that are welded or shot-fired onto the steel section and embedded in the concrete slab.

The load carrying capacities of shear connectors in the room temperature can be designed according to BS 5950: Part 3 (BSI 1990), Eurocode 4: Part 1.1 (BSI 2004) and AS 2327 (Standard Australia 1996). For the shear connectors embedded in composite slabs with profiled steel deckings, a reduction factor is formulated to include the effects of trough shapes of deckings/slabs on load carrying capacities of shear connectors. Two failure mechanisms are normally considered in practical design, namely:

1) yielding of shear connectors; and
2) crushing and splitting of concrete materials in close vicinity to shear connectors.

While under the fire limit state, the load carrying capacities of shear connectors can be assessed

*Corresponding author, Ph.D., E-mail: aaron.juan.wang@gmail.com

according to Eurocode 4: Part 1.2 (BSI 2005). A reduction factor is applied considering the reduction in material strength of both shear connectors and concrete slabs. According to Eurocode 4: Part 1.2 (BSI 2005), the reduction factor can be taken as the smaller value between that of the concrete and 0.8 times of the reduction factor for the steel.

1.1 Experimental investigations

A large number of push-out tests have been conducted under cool state over the past three decades on shear connectors embedded in solid slabs (Ollgaard *et al.* 1971, Johnson and Oehlers 1981, Oehlers and Johnson 1987). Based on the results of these experimental investigations, simple design rules are proposed towards load carrying capacities of shear connectors embedded in solid slabs. Normalized load-slippage curves were also proposed to predict the load-slippage characteristics of headed stud shear connectors in concrete slabs (Ollgaard e*t al.* 1971). Mattran and Johnson (1990) conducted a series of push-out tests on shear connectors embedded in composite slabs with profiled steel deckings. Steel deckings of different profiled shapes were included in the study. The interaction of stresses due to adjacent shear connectors in the same trough was also studied. A modified formation of the standard self-drilling screw in the beam-to-sheet connection is proposed as shear connectors in the recent research done by Erdelyi and Dunai (2009). Push-out tests were conducted to study the composite behaviour of the different connection arrangements. The design rules have been developed accordingly to predict both the stiffness and load carrying capacities of the new type of shear connectors.

A comprehensive experimental investigation into the structural behaviour of composite beams and shear connectors under the standard fire was conducted by Zhao and Kruppa (2002a, b). Push-out tests were conducted on both headed and angle shear connectors embedded in both solid and composite slabs at elevated temperatures. Various profile shapes of steel deckings are covered including both trapezoidal and re-entrant types. Normalized load-slippage curves of shear connectors at elevated temperatures were formulated based on test results for practical design.

1.2 Numerical investigations

A two-dimensional finite element model was proposed by Kim *et al.* (2001), in which plane stress elements were adopted to simulate the composite slabs, steel beams and shear connectors, while steel deckings are modelled with beam-column elements. With the careful definition of equivalent widths of shear connectors and composite slabs, the three-dimensional stress and strain behaviour in push-out tests were simplified into a two-dimensional problem. The model was verified to be able to predict load-slippage behaviour of shear connectors at service loads through the calibration against test data. Lam and El-Lobody (2005) propose a three-dimensional finite element model for push-out tests of headed shear connectors in solid slabs. Three-dimensional solid elements were used to simulate both concrete slabs and shear connectors. It was assumed that concrete exhibits a quite ductile behaviour with the provision of sufficient local reinforcement, so that local concrete crushing and cracking can be efficiently eliminated. Hence, von Mises failure criteria was adopted for the material model of concrete without the consideration of local concrete crushing and tension softening. The results of the proposed model were found to compare well with tests data in terms of load-slippage characteristics.

Wang (2009) proposed a three-dimensional finite element model to examine the structural

behaviour of shear connectors in push-out test specimens with different geometries and under various loading and boundary conditions. Von Mises failure criteria was adopted for the steel material simulation, while Drucker-Prager failure criteria was adopted for the concrete material modelling. Micro concrete cracks were also incorporated using a smear cracking model. The proposed three-dimensional finite element model was verified to be able to predict accurately the load carrying capacities and the load-slippage characteristics of shear connectors in various types of slabs at a small to mediate slippage not exceeding 4 mm. However, the non-ductile deformation characteristics of the shear connectors due to extensive concrete cracks at large deformation cannot be modelled by the proposed three-dimensional finite element models. This was because of the limitation of the material model for the concrete.

2. Objectives and scope of work

This paper aims to study structural and thermal response of shear connectors under elevated temperature though numerical approaches. Three-dimensional thermal-mechanical coupled finite element models are proposed to study the structural behavious of shear connectors under fire with the full incorporation of thermal, mechanical and geometrical non-linearities. Specimens of both solid and composite slabs are studied. The objectives of this research paper include:

1) To propose three-dimensional thermal-mechanical coupled finite element models to study the structural behavious of shear connectors under fire with the full incorporation of thermal, mechanical and geometrical non-linearities.

2) Through studying the development of sectional temperature fields as well as internal forces and moments from the numerical modelling, further details on the thermal and structural response of shear connectors under fire are to be revealed, which leads to a better structural understanding.

3. Finite element models

Nonlinear three-dimensional finite element thermal-mechanical coupled models were set up using the commercial finite element package ABAQUS (2006) to study the thermal and structural response of shear connectors in push-out tests under elevated temperatures.

3.1 Finite element mesh

The meshes of the finite element models are shown in Fig. 1(a) for specimens of solid slabs and Fig. 1(b) for specimens of composite slabs. Concrete slabs, steel beams and shear connectors are modelled with eight-noded solid elements. In order to simplify the problem and save computational effort, only one quarter of the specimen was modelled.

More than 8 elements are arranged in the longitudinal direction of shear connectors with a typical element size of $10 \times 10 \times 10$ mm. The elements in the concrete slabs around the shear connectors are also locally refined. A mesh sensitivity and convergence study was conducted and presented in Fig. 2. It is found that the curvature due to the dowelling effects and the flexural bending of shear connectors can be modelled accurately with such element arrangement. Local thermal and
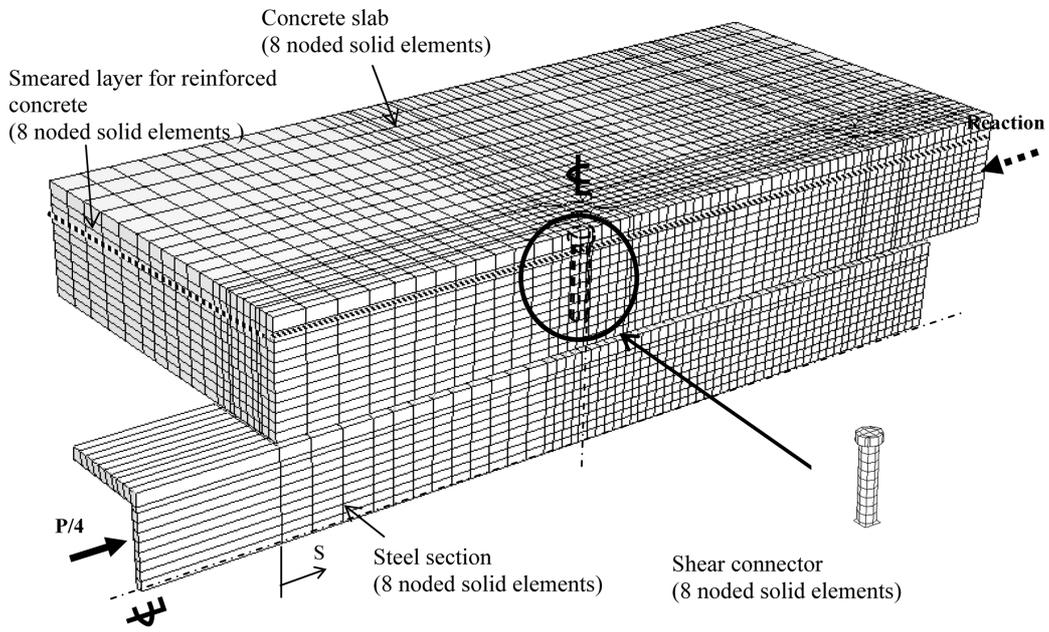
(a) Push-out tests with solid slabs
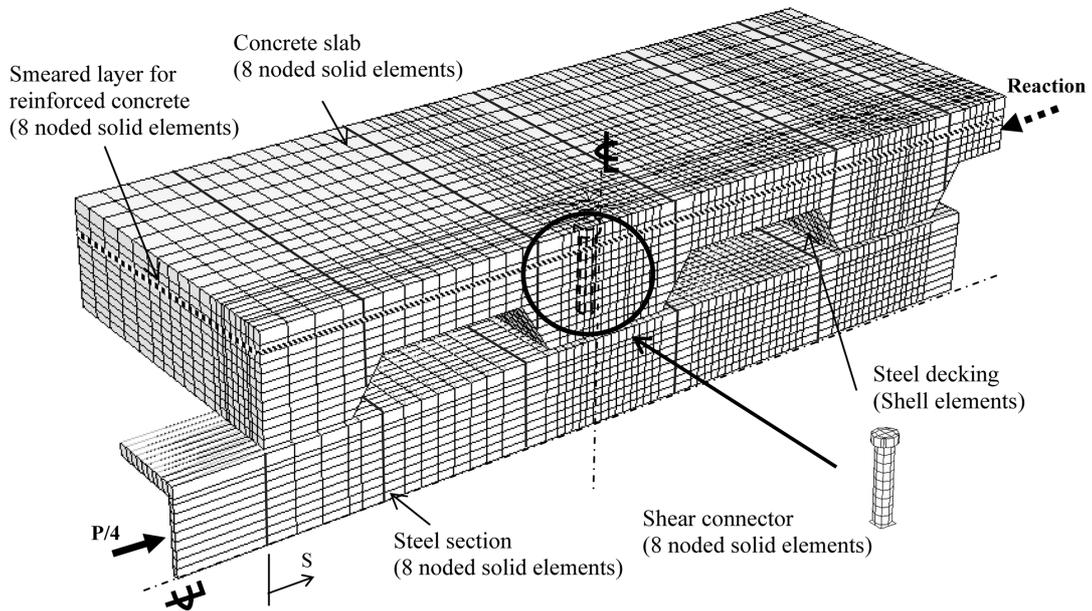
(b) Push-out tests with composite slabs

Notes:
1)   Both finite element thermal and mechanical models share the same set of mesh.
2)   Only one quarter of the test set-up is modelled due to symmetry.
3)   Contact elements are not shown for clearity.
4)   Thermal flux is input from the steel beam and bottom of the slab considering the shadow effects.

Fig. 1 Three-dimensional finite element thermal and mechanical models for push-out tests
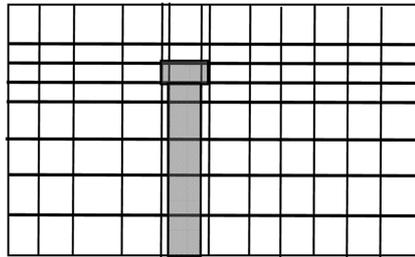
i) Mesh A
(Typical element size: 20 x 20 x 20 mm)
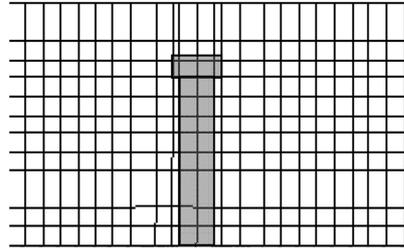
ii) Mesh B
(Typical element size: 10 x 10 x 10 mm)
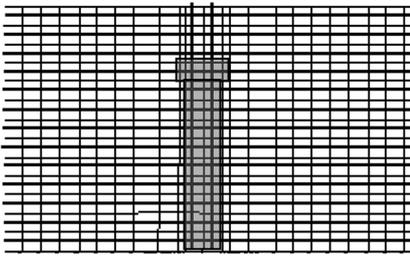
iii) Mesh C
(Typical element size: 5 x 10 x 10 mm)

Geometrical data:
- Slab depth, D_s = 150 mm
- Area of reinforcement, A_s = 393mm2
- 19 mm headed shear connector of 100 mm height is adopted.

Material data:
- Cylinder concrete strength, f_c = 40 N/mm^2
- Yield strength of shear connector, f_y = 460 N/mm^2

One shear connector is adopted in the analysis.
Thermal analyses are conducted under a standard fire.
Mechanical analyses are conducted in room temperature.

(a) Different arrangements of finite element mesh
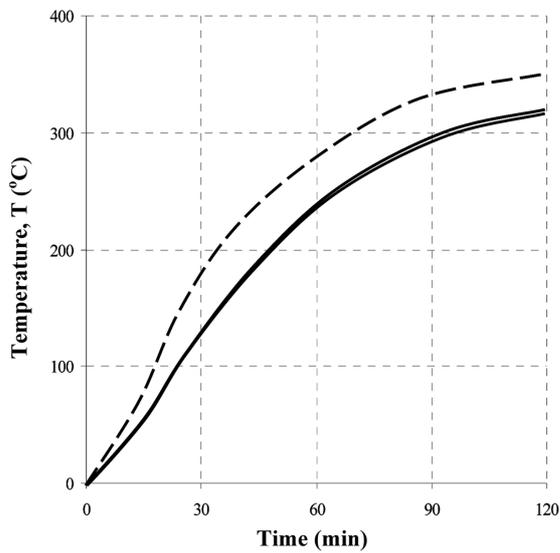
(b) Time-temperature curves at the top of a shear connector under thermal analyses
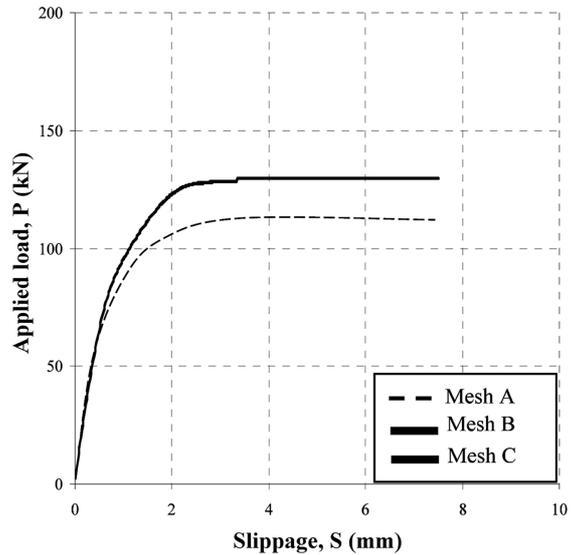
(c) Load-slippage curves for a specimen under mechanical load

Fig. 2 Mesh sensitivity and convergence study

mechanical contact condition between the shear connectors and the surrounding concrete can also be modelled accurately. The concrete crushing and splitting due to stress concentration can be incorporated as well with the proposed finite element mesh arrangement.

It should be noted that, since the analyses are coupled ones, both the finite element thermal and mechanical models share a same set of finite element mesh while with different element types. Thus, the nodal temperature fields and histories as predicted by the thermal model can be easily adopted by the mechanical model at each of the time steps, and the deformed mesh due to mechanical loading and material softening can also be updated in the thermal analysis in the same time step.

3.2 Finite element thermal modelling

Concrete slabs, shear connector and steel sections are modelled with three-dimensional quadratic solid elements, DC3D10, with different thermal properties. Profiled steel deckings were modelled with three-dimensional quadratic shell elements, DS8. The material thermal properties of both concrete and steel materials are adopted from Eurocode 4: Part 1.2 (BSI 2005) and also shown in Table 1 for easy reference. A layer of contact elements are provided at the interface of the concrete slab and the steel section, and the thermal conductivity of these contact elements is assumed to be 0.3 W/k/m^2. The same layer of contact elements are also provided at the interface of the shear connector and the surrounding concrete elements. The thermal fluxes due to both radiation and convection of the standard fire in Eurocode 1 Part 1.2 (BSI 2002) are adopted, and they are given by

$$h_{\text{net},r} = \phi\xi_{\text{res}}\, 5.67 \times 10^{-8}[(\theta_f + 273)^4 - (\theta_m + 273)^4] \tag{1}$$

$$h_{\text{net},c} = \alpha_c(\theta_f - \theta_m) \tag{2}$$

where

$h_{\text{net},r}$, $h_{\text{net},c}$ are the radiation heat flux and the convection heat flux respectively;

θ_f is the furnace gas temperature and usually follows the standard fire temperature curve (BSI 2002);

ϕ is the configuration factor, and is taken to be 1.0 conservatively;

ξ_{res} is the resultant emissivity of the exposed surface and is taken as 0.8 as suggested in Eurocode 1: Part 1.2 (BSI, 2002);

Table 1 Typical material thermal property

| Property	Steel	Normal weight concrete	Fire protection material
Density, ρ (kg/m^3)	7850	2300	800
Specific heat, c (J/kg °C)	600	1000	625
Thermal conductivity, λ (W/m °C)	45	1.6	0.15
Coefficient of expansion, α ($\times 10^{-6}$)	14	18	-
Latent heat of water		2.25×10^6 J / kg	
Energy absorption due to water evaporation for a moisture content of concrete at 4%		2.25×10^6 J / kg $\times$ 4% $= 9.0 \times 10^4$ J / kg of concrete	
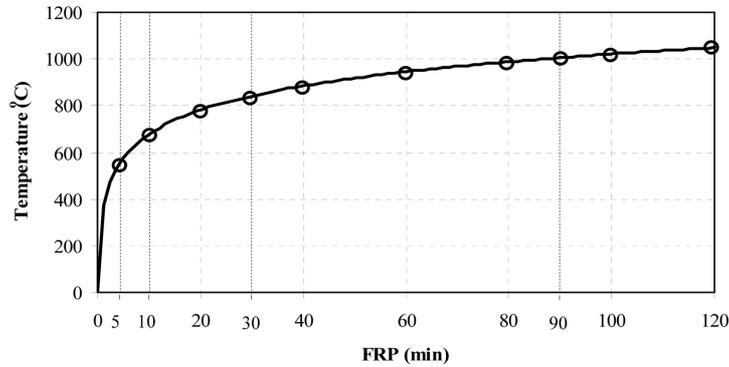
Fig. 3 Standard fire temperature curve (BSI 2002)

α_c is the coefficient of heat transfer by convection;
= 25 W/m^{2}K on the side exposed to fire; and
= 9 W/m^{2}K on the side exposed to air.

The standard fire temperature curve is adopted as shown in Fig. 3, and can be expressed as follows according to Eurocode 1: Part 1.2 (BSI 2002).

$$\theta_f = 20 + 345 \log_{10}(8t + 1) \tag{3}$$

where
t is the time elapsed in minutes.

It should be noted that both options SFILM and SRADIATE are used to model the radiation and the convection heat fluxes respectively. The shadow effects due to flanges of steel sections were considered by applying a reduction factor to the total heat flux (BSI 2004), which is given by

$$k_{\text{shadow}} = 0.9 \times \frac{2T + 0.5B + d}{d + 1.5B + 2T - t} \tag{4}$$

where
T is the thickness of steel flanges;
t is the thickness of steel webs;
B is the width of steel flanges; and
d is the depth of steel webs.

The latent heat energy in concrete flanges is also incorporated with a specified moisture content of 4% within the concrete mass. As shown in Table 1, the overall latent heat energy for water is taken to be 9.0 × 10^4 J/kg of concrete with a moisture content of 4%. The latent heat energy loss due to moisture evaporation in concrete is modeled by the option LATENT HEAT in ABAQUS (2006) and evaporation of free water is assumed to take place from 90ºC to 110ºC in order to avoid numerical divergence.

3.2 Finite element mechanical modelling

Concrete slabs, steel beams and shear connectors are modelled with eight-noded solid elements, C3D8. The elements in concrete slabs around shear connectors are also locally refined so that local concrete crushing and splitting due to the interaction between shear connectors and surrounding concrete can be captured. Reinforcement is also simulated with the same type of solid elements and assumed to be bonded perfectly to its surrounding concrete. Profiled steel deckings of composite slabs are modelled with eight-noded double curvature shell elements, S8. It is assumed that steel deckings are mechanically bonded perfectly to concrete slabs, so that there is no relative slippage between steel deckings and concrete slabs.

Spring contact elements with large compressive stiffness and zero tensile stiffness are placed between shear connectors and their surrounding concrete so that local interaction between them can be simulated accurately. The same type of contact spring elements are placed between the bottom of slabs and the top surface of steel flanges to model the interaction between slabs and steel sections. The value of the contact stiffness is assigned to be 20000 N/mm after a trial-and-error process in comparing the measured and the predicted time or load-slippage curves of a number of test specimens, and the value of contact stiffness are assumed to remain constant throughout the analysis.

The reduction in strength and stiffness of both concrete and steel materials at elevated temperature is taken from relevant clauses in Eurocode 4: Part 1.2 (BSI 2005), which is also shown in Fig. 4 for easy reference. The thermal expansion coefficients of steel and concrete materials are taken to be 14×10^{-6} and 18×10^{-6} respectively according to Eurocode 4: Part 1.2 (BSI 2005) for simplicity.

A multi-linear stress-strain curve is adopted for the steel, as shown in Fig. 5(a). The failure of steel sections and shear connectors follows von-Mises failure criteria whose failure surface is shown in the same figure. The steel material is specified to reach its yield and ductility limits at the limiting strain of 0.15 and 0.2 respectively. A non-linear stress-strain curve is adopted in the material model of concrete under uni-axial loading condition, as shown in Fig. 5(b). Crushing is
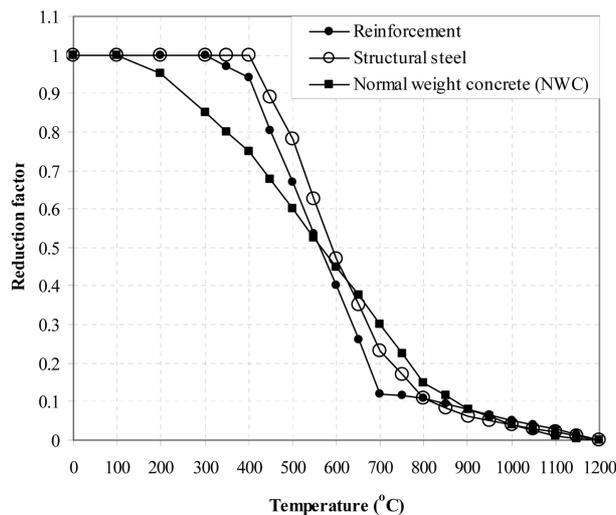

Fig. 4 Strength reduction factors (BSI 2005)

(a) Steel
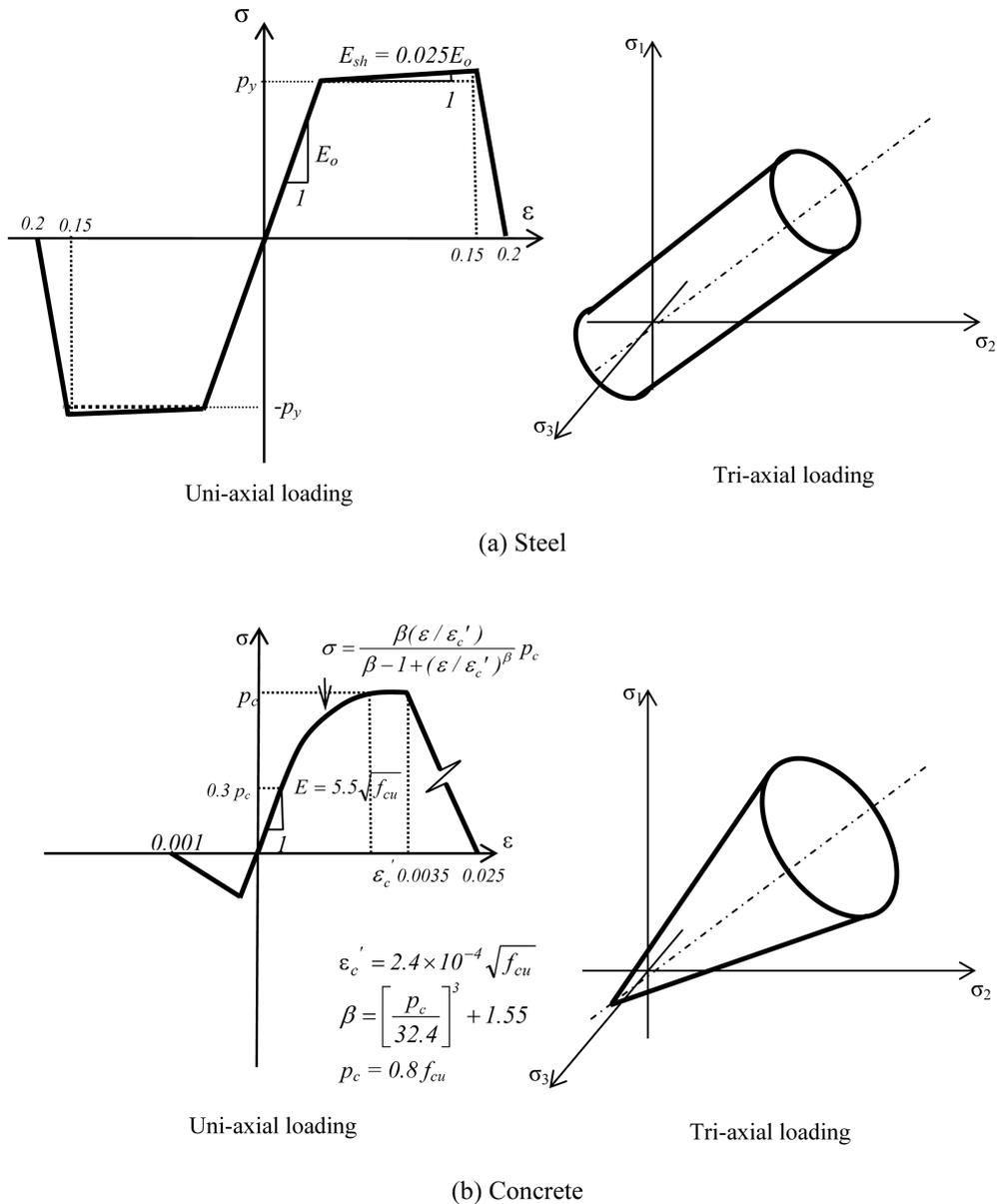
(b) Concrete

Fig. 5 Material models

included in the material model of concrete through the uni-axial definition of stress-strain curves for the concrete material under tri-axial compression. The failure surface of concrete material follows the Drucker-Prager failure criteria (ABAQUS 2006) as presented in Fig. 5(b). The friction angle of the concrete is taken as 67.5° for $p_t/p_c = 0.1$, where is p_t is the uni-axial tensile strength, and p_c is the cylinder strength. Micro-cracking in the concrete slabs is simulated with a smeared cracking model. The tensile strength of concrete is taken as 10% of its compressive strength and assumed to reduce linearly from its peak value to zero at the tensile strain of 0.1% as shown in Fig. 5(b).

3.3 Solution procedure

In the current investigation, the analyses are conducted through a series of time steps in the total fire resistant period. In each of the time step, the numerical thermal analyses are conducted first under a specified thermal flux. The thermal non-linearities are also incorporated in order to simulate the effects of the latent heat due to the moisture evaporation. The applied mechanical loads are kept to be constant all through the analysis, while the temperature field adopted in mechanical analyses is from the nodal temperatures generated by the thermal analyses at each of the time step. A value of 5% is recommended as the maximum plastic strain increment in each time step. In order to accurately model the large deformation at critical locations after steel yielding as well as local concrete crushing and splitting, both material and geometrical non-linearities were incorporated into the finite element model. Thus, both the thermal and mechanical analyses are coupled in each of the time step, and the deformation of the finite element mesh due to the mechanical loading and material softening is able to be incorporated into the thermal analysis. This is especially important during the large deformation stage near failure when the geometrical configuration near the shear connector has been changed a lot with extensive yielding and concrete crushing and splitting, which may alter the heat transfer pattern in the failure region.

As this is a highly nonlinear problem, the solution is obtained through a number of equilibrium interactions for each time step. This is accomplished by an arch-length procedure, in which the maximum arch-length intergrading time interval and the corresponding nodal displacement is monitored and controlled in each equilibrium interaction so that no numerical divergence happens. The nodal displacements, the out-of-balance forces and the tangent stiffness matrix of the structure are updated after each equilibrium interaction. A force-based convergence criteria is adopted which requires the imbalance force is less than 0.5% of average applied force in each equilibrium interaction. The overall iteration and computation process for typical thermal and mechanical models takes roughly 20 minutes on an ordinary personal computer.

4. Numerical results

To ensure the general applicability of the proposed finite element models, 4 push-out tests under either room temperature or the standard fire conducted by Zhao and Kruppa (2002) with fully documented test results covering practical parameters are selected for the calibration of the finite element models. Table 2 presents general information of these push-out tests and the material properties of both steel and concrete sections are presented in Table 3. Fig. 6 shows the typical setup of a push-out test under fire. The detailed loading, boundary and thermal conditions as well as geometrical configurations of these tests are presented in Figs. 7 to 9. Shear connectors in both solid and composite slabs are covered in the current study. Different types of profile steel decking of trapezoidal and re-entrant types are both considered. In addition, different amounts of tensile reinforcement in the concrete slabs are also covered. It should be noted that all the specimens were tested under the standard fire with the constant applied loads except Specimen Solid-1, which was tested in the room temperature under a gradually applied increasing load as a reference specimen.

The nominal yield strength of the steel sections and the shear connectors are typically 311 N/mm^2 and 460 N/mm^2, respectively, while the measured cylinder strengths of concrete range from 34.5 MPa to 43.3 MPa. All of the push-out tests are terminated due to excessive slippage between

Table 2 Summary of push-out tests

Test	Test in the room temperature/ standard fire test	Type of slab	Type of profile steel section	Number of shear connectors per trough	Thickness of profiled steel decking, t_d (mm)	Slab depth, D_s (mm)	Area of reinforcement (mm^2)
Solid-1	Test in room temperature	Solid slab	-	2	-	130	393
Solid-2	Standard fire test	Solid slab	-	2	-	130	393
Comp-1	Standard fire test	Composite slab	Trapezoidal	2	0.9	130	142
Comp-2	Standard fire test	Composite slab	Re-entrant	2	0.9	130	142

Note:
1) All shear connectors are 19 mm headed shear connectors of 100 mm height.
2) The depth of all slab are 130 mm.
3) The thickness all steel deckings is 0.9 mm.

Table 3 Strengths of specimens in push-out tests

| Test	Nominal yield strength of steel beam (N/mm^2)	Nominal yield strength of shear connectors (N/mm^2)	Measured cylinder strength of concrete (N/mm^2)
Solid-1	311	460	34.5
Solid-2	311	460	34.5
Comp-1	314	460	43.3
Comp-2	314	460	43.3

steel sections and concrete slabs with extensive crushing and visible cracks in close vicinity to stud shear connectors. The numerical results of the finite element analyses are presented and discussed in the following sections.

4.1 Results from the thermal analyses

The temperature fields obtained from the finite element analyses for Specimens Solid-2, Comp-1 and Comp-2 are presented in Fig. 10 for the fire resistant periods of both 1 hr and 2 hrs. A close observation on the numerical results reveals that, due to the relatively high thermal conductivity of the steel material, the temperature in shear connectors are typically 100 to 150°C higher than that of the surrounding concrete elements.

Fig. 11 presents the time-temperature curves at the both the top and bottom of the shear connectors. The results from the tests are also plotted in the same figure for a direct comparison. It can be seen that both the numerical and experimental results compare well with each other, and the numerical modelling provides slightly more conservative results as compared with the test results. It is also noted that the temperature at the bottom of the shear connectors is typically 500 and 350°C higher than the top of the shear connectors for the fire resistant periods of 1 hr and 2 hrs respectively. The temperature difference up to this scale may lead to the failure of the shear

Fig. 6 Typical setup of a push-out test under fire
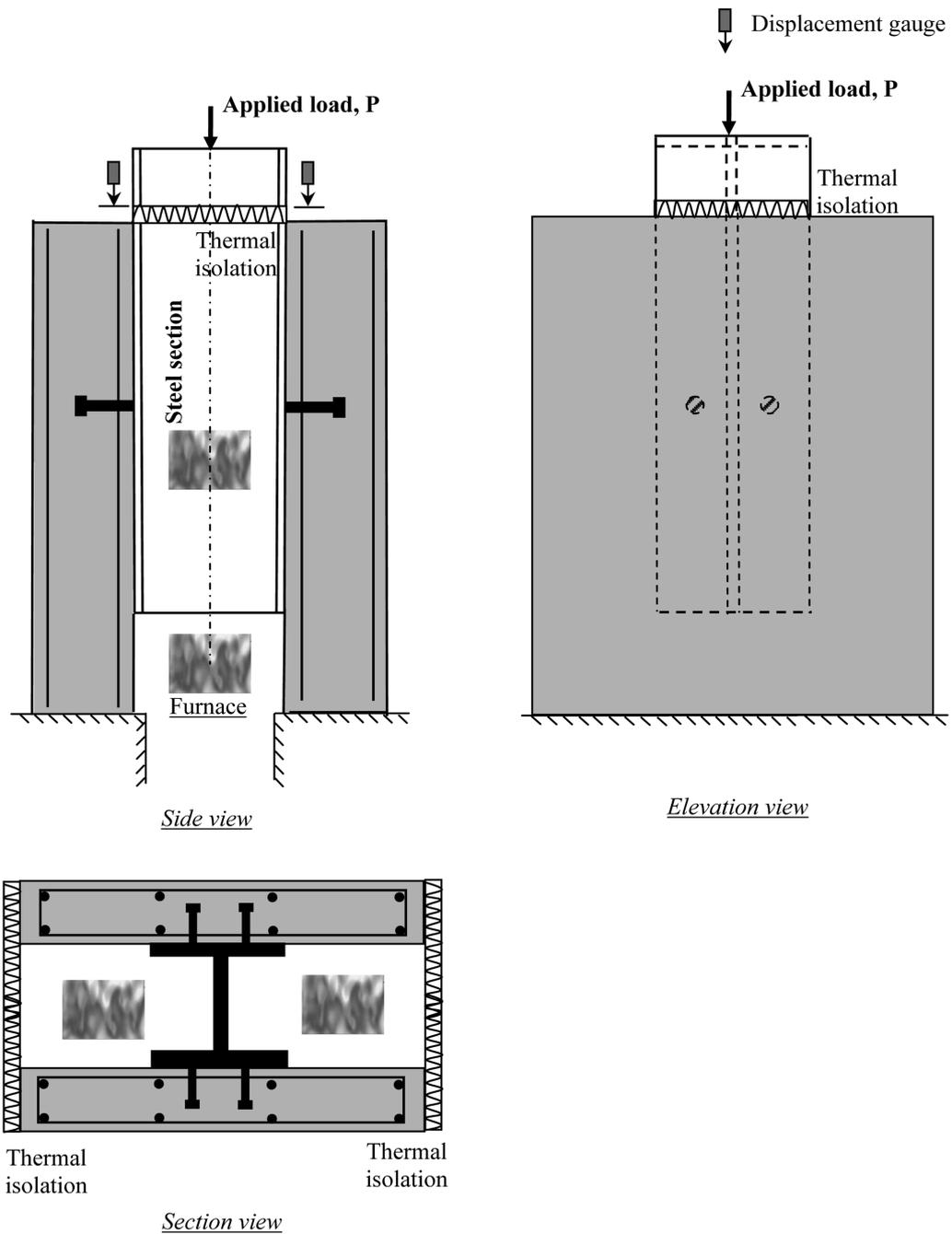
Note:
1)   The rebars in the concrete slab are not shown in the elevation view for clarity.
2)   The displacement of the steel section relative to the concrete slab is measured through displacement gauges attached at various positions on test specimens.

Solid −1. tested in the room temperature.
Solid −2. tested under the standard fire.
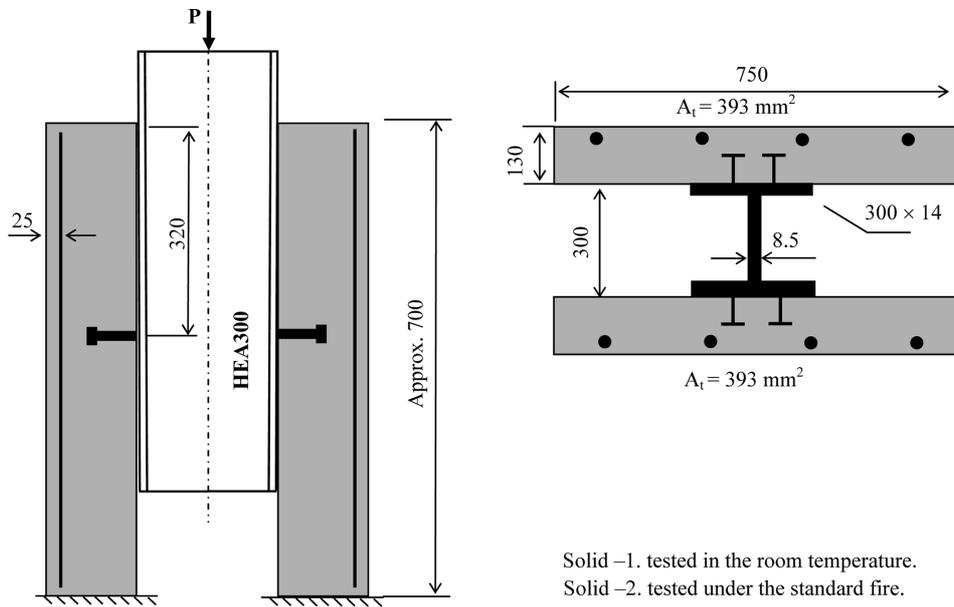
Note:
All shear connectors are 19 mm headed shear connectors.

Fig. 7 Specimens Solid-1 and Solid-2 (Details refer to Zhao and Kruppa 2002)
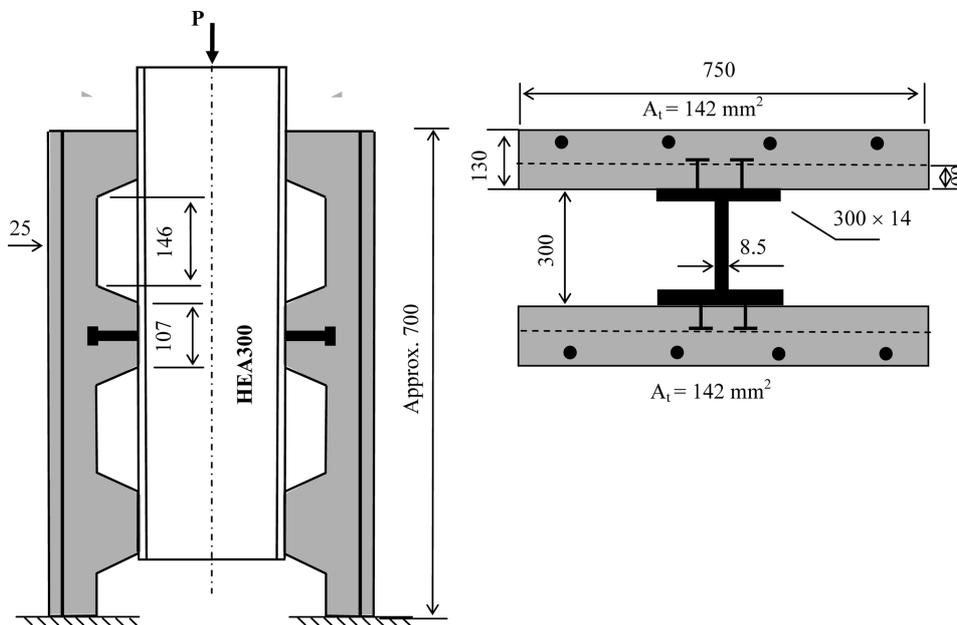

Note:
All shear connectors are 19 mm headed shear connectors.

Fig. 8 Specimen Comp-1 (Details refer to Zhao and Kruppa 2002)
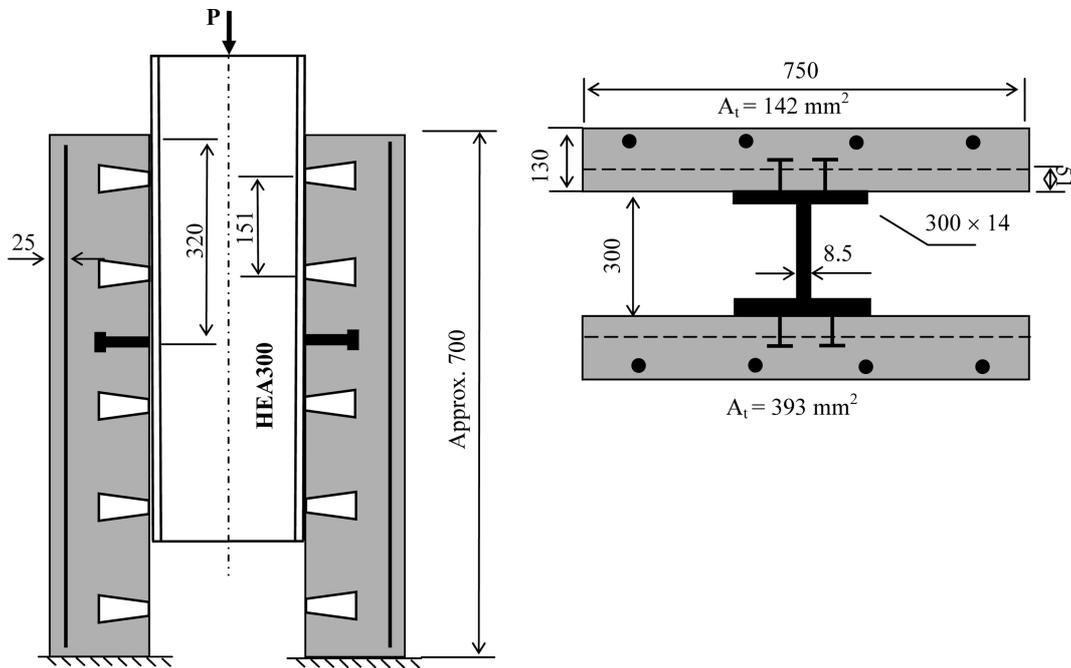
Note:
All shear connectors are 19 mm headed shear connectors.

Fig. 9 Specimen Comp-2 (Details refer to Zhao and Kruppa 2002)

(a) Solid-2

(b) Comp-1

(c) Comp-2
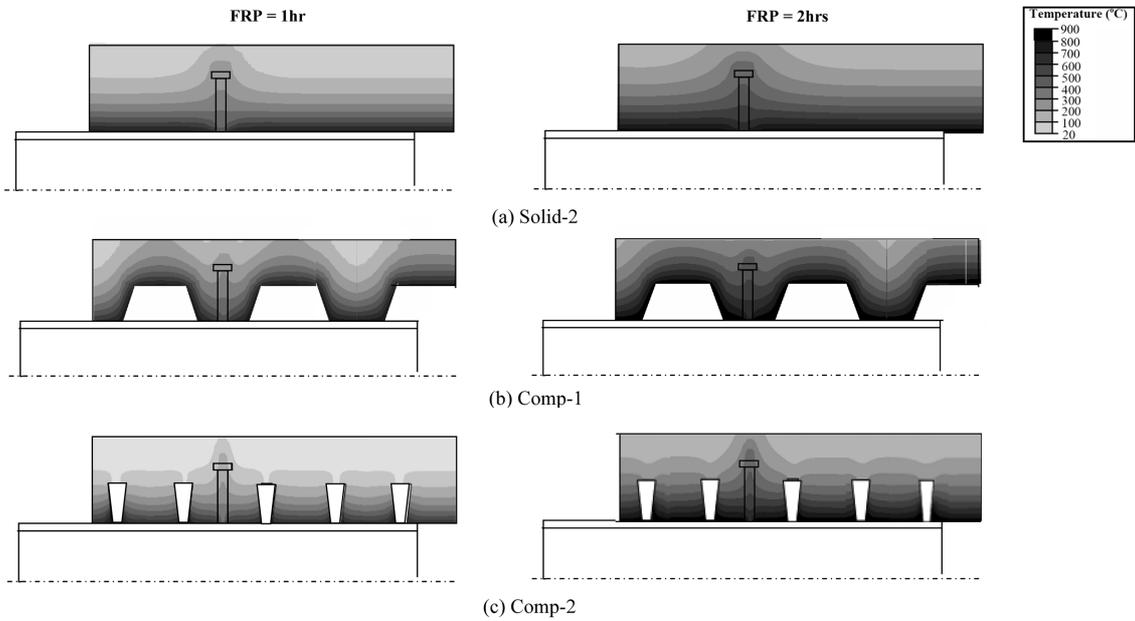
Note: Temperature is plotted in the section along the center lines of the shear connectors

Fig. 10 Temperature field in concrete slabs and shear connectors

(a) Solid-2

(b) Comp-1

(c) Comp-2
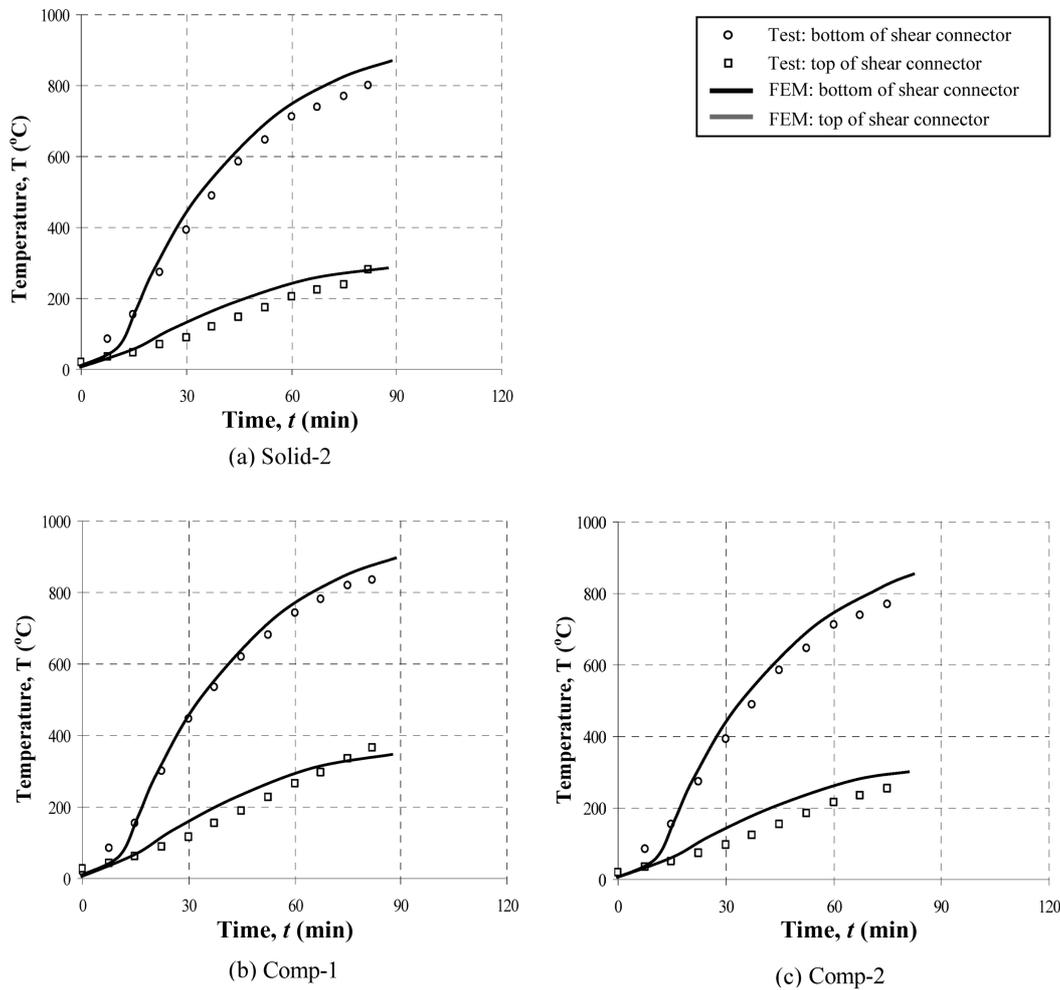
Fig. 11 Time-temperature curves

connectors due to material softening and excessive slippage.

4.2 Results from the mechanical analyses

Fig. 12(a) presents load-slippage curves obtained from the finite element analysis on Specimen Solid-1 in the room temperature, while the time-slippage curves from Specimens Solid-2, Comp-1 and Comp-2 under the standard fire are plotted in Figs. 12(b)-(d). The test results are also plotted in the same figures for direct comparison. It is shown that both of the approaches give quite close results, which verifies the accuracy of the proposed finite element models.

Negative placements are recorded in both physical tests and numerical analyses. This is due to the relatively high thermal expansion as compared with the deformation due to mechanical loads in the initial stages of the standard fire tests. As the behavior of the negative displacement relies heavily on the thermal expansion performance of both concrete and steel materials, different levels of thermal expansion coefficients are taken in the finite element modelling, say $0.9\alpha_e$ and $1.0\alpha_e$, where

(a) Solid-1

(b) Solid-2

(c) Comp-1

(d) Comp-2
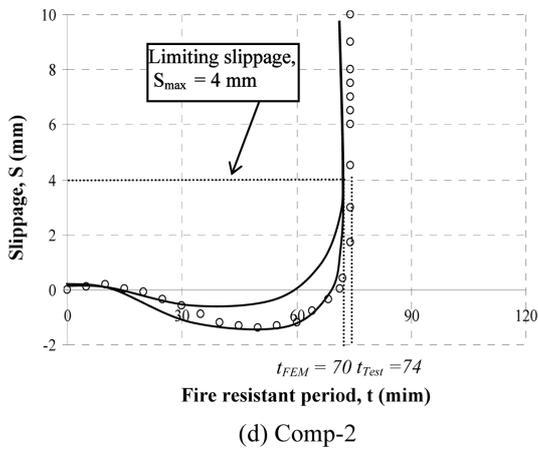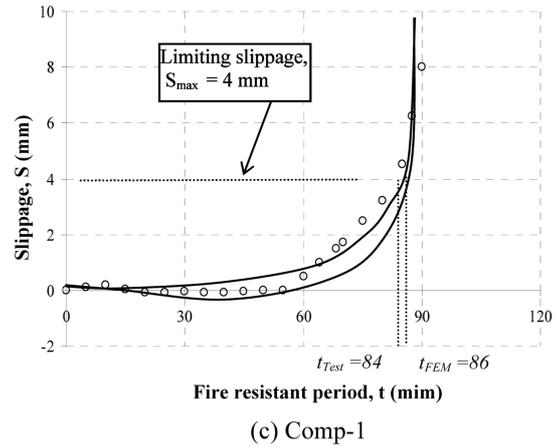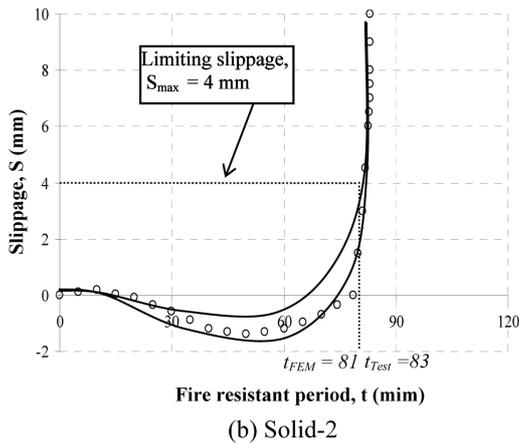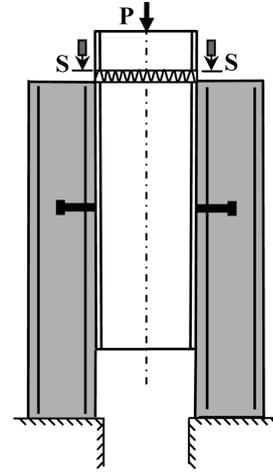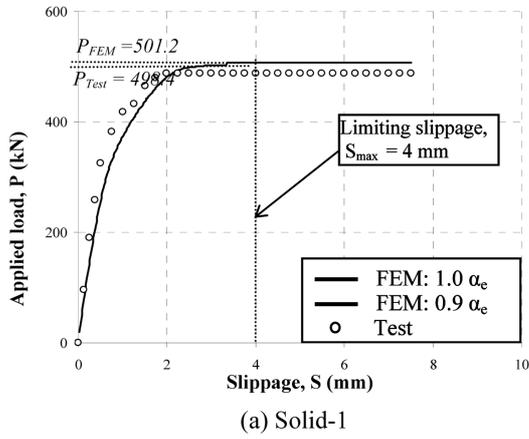
Fig. 12 Time-slippage curves

Table 4 Fire resistant periods of specimens in push-out tests

| Test	Test			Eurocode 4: Parts 1.1 and 1.2		Finite element modelling		Model factor	
	Load carrying capacity in the room temperature, P_{Test} (kN)	Load ratio in fire test	Fire resistant period, t_{Test} (min)	Load carrying capacity at room temperature, P_{EC} (kN)	Fire resistant period, t_{EC} (min)	Load carrying capacity at room temperature, P_{FEM} (kN)	Fire resistant period, t_{FEM} (min)	t_{Test}/t_{EC}	t_{Test}/t_{FEM}
Solid-1	498.4	-	-	360.1	-	501.2	-	-	-
Solid-2	501.2	0.4	83	360.1	77	-	81	1.08	1.02
Comp-1	352.5	0.4	84	388.3	82	-	86	1.02	0.98
Comp-2	385.4	0.6	74	403.4	67	-	70	1.10	1.06
Average								1.07	1.02

α_e is the thermal expansion coefficient according to Eurocode 4: Part 1.2 (BSI 2005). As can be seen from Figs. 12(b)-(d), different levels of thermal expansion coefficients lead to a difference in maximum negative displacement up to 1 to 1.5 mm. A close observation on the thermal expansion behavior of the test specimens also reveals that the amount of the thermal expansion for specimens with solid slabs (Specimen Solid-2) and with composite slabs of re-entrant steel decking (Specimen Comp-2) is 1.5 to 1.8 mm larger than the specimen with composite slabs of trapezoidal steel decking (Specimen Comp-1). This is possibly because the concrete volume of Specimen Comp-1 is significantly lower than that of both Specimens Solid-2 and Comp-1 due to the voids between adjacent troughs provided a same slab thickness, and it is well understood that the amount of thermal expansion depends heavily on volumes of the concrete mass.

For back analysis purpose, the load carrying capacities predicted by the proposed finite element model in the room temperature are defined to be equal to the load level or the time rating at a limiting slippage, S_{max} of 4 mm. This amount of slippage is normally considered to be large enough to fully mobilize the shear resistances of typical headed shear connectors (BSI 1990, Patrick 2000, Hegger and Doingha 2002). Table 4 presents both the measured and predicted load carrying capacities for Specimen Solid-1. The load carrying capacity calculated according to the design formulae in Eurocode 4: Part 1.1 (BSI 2004) is also presented in the same table for direct comparison and reference. A comparison on measured and predicted values shows that the proposed finite element model is able to provide accurate prediction on the load carrying capacities of shear connectors in the room temperature. While Eurocode 4: Part 1.1 (BSI 2004) is still considered to be effective in providing relatively conservative results.

Similarly, the fire resistant period for a specimen tested under the standard fire is also taken to be the time elapsed at the limiting slippage of 4 mm (BSI 1990, Patrick 2000, Hegger and Doingha 2002). It is noted from Table 4 that the average model factor of the proposed three-dimensional finite element models is 1.02 while that of the design rules in Eurocode 4: Part 1.2 (BSI 2005) is 1.07. It is demonstrated that the proposed finite element models can provide accurate prediction to the fire resistant periods of the shear connectors under the standard fire. The design rules in Eurocode 4: Part 1.2 (BSI 2005) are also considered to be effective in predicting conservatively the fire resistant periods of the shear connectors at various applied load levels.

4.3 Failure modes

Fig. 13 presents the distribution of stresses in the concrete material at the failure of the specimens. As shown in Fig. 13(a) for Specimen Solid-1 tested in the room temperature, the maximum stress occurs near the bottom of the concrete slab. While for Specimens Solid-2 and Comp-2 tested under the standard fire tests, the maximum stress occurs at 35 to 45 mm from the bottom of the slabs due

(a) Solid-1

(b) Solid-2

(c) Comp-1

(d) Comp-2
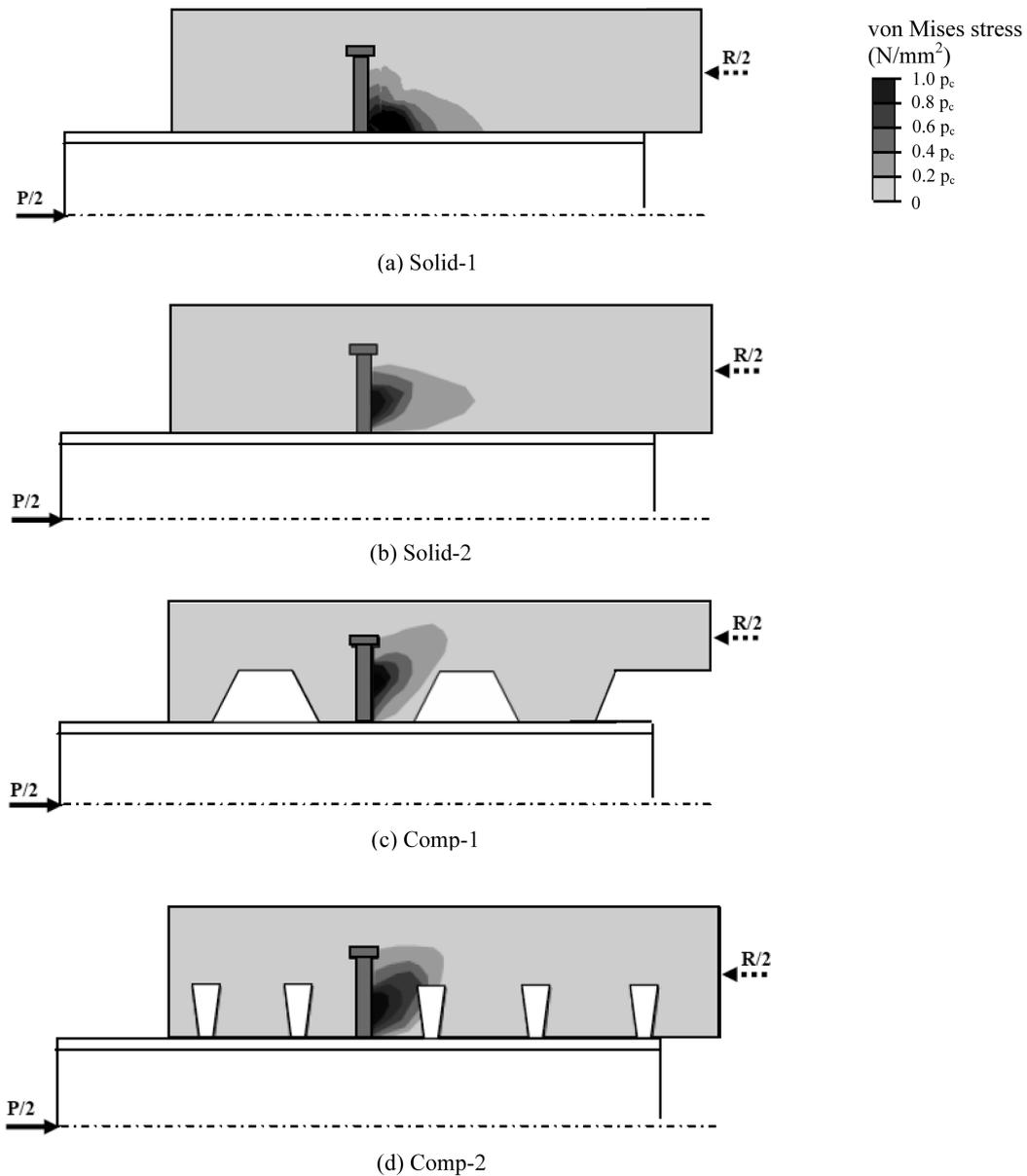
Note: Stress is plotted in the section along the center lines of the shear connectors

Fig. 13 Stress distributions in concrete at failure

(a) Solid-1

(b) Solid-2


(c) Comp-1

(d) Comp-2
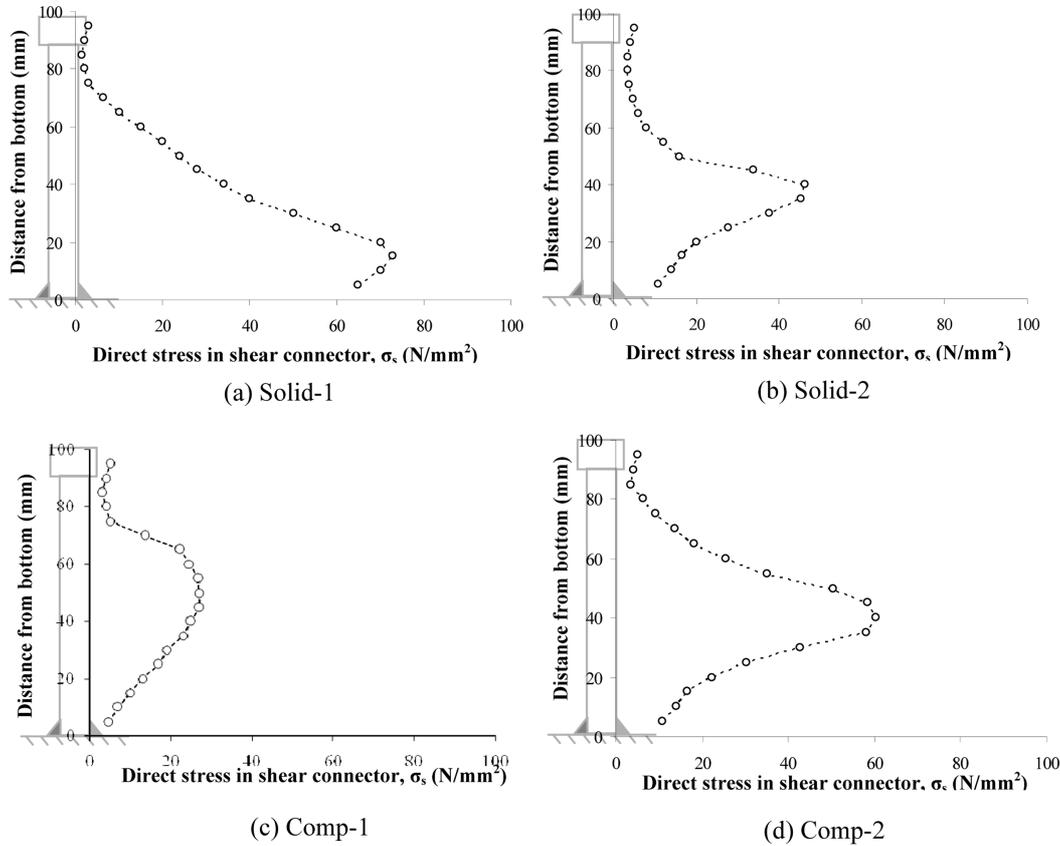
Fig. 14 Distributions of direct stress in shear connectors at failure

to the reduced material strength at the bottom layers of the concrete under relatively high temperatures. For Specimen Comp-1 with composite slabs with trapezoidal steel decking, due to the voids between adjacent troughs, the temperature in the trough is even higher as compared with the case for Specimen Comp-2, the location of concrete stress concentration further shifts upwards to 55 mm from the bottom of the slabs. Similar phenomena can also be observed in Fig. 14, where direct stresses on the shear connectors are plotted at failure.

Fig. 15 plots the deformed shape on the shear connectors in each of the test specimens. As can be seen from Figs. 15(a), 15(b) and 15(d), due to relatively low location of stress concentration, the 'shearing-off' type failure modes are observed. While for Specimen Comp-2 in Fig. 14(c), the maximum stress concentrated at a higher position of roughly 55 mm from the bottom of the shear connectors, which generates a relative large over-turning moment about the bottom of the shear connector as combined with the bottom shear load. Thus, failure occurred in an 'over-turning' mode with a reduced load carrying capacity. Another reason for this failure mode is that the temperature profiles in the shear connector is normally 100 to 150°C higher that the surrounding concrete as discussed in Section 4.1, which leads to a faster deterioration in the shear connectors as compared with the surrounding concrete, and the failure mode switches from the crashing and splitting of the surrounding concrete as commonly understood to the yielding and over-turning of the shear connector itself.
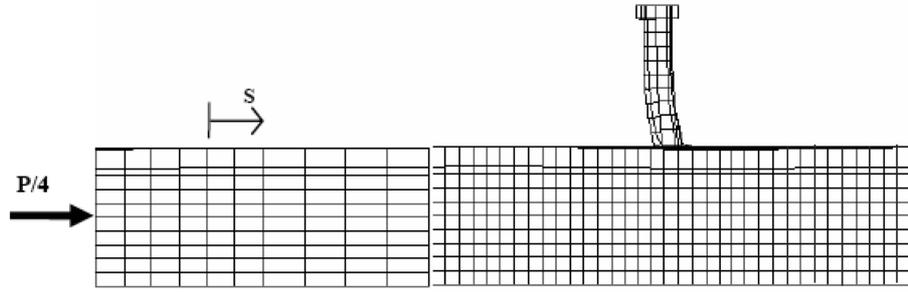
(a) Solid-1
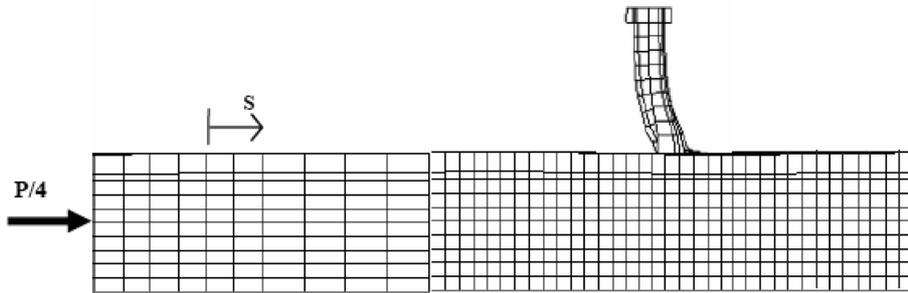
(b) Solid-2
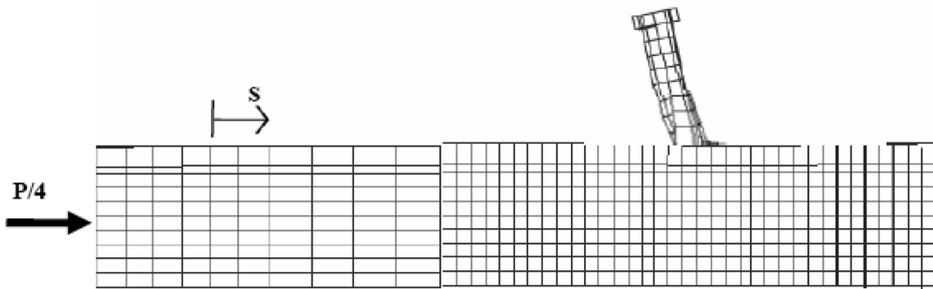
(c) Comp-1

(d) Comp-2

Fig. 15 Deformed shape of push-out test specimen

5. Conclusions

Three-dimensional thermal and mechanical coupled finite element models are proposed to study the structural behavious of shear connectors under fire. Various nonlinearities including thermal, mechanical and geometrical nonlinearities are also incorporated. The accuracy of the models is verified through the validation against a series of push-out tests either in the room temperature or under the standard fire. Various thermal and mechanical responses are also extracted and observed in details from the results of the numerical analyses, which gives a better understanding of the structural behavior of shear connectors under elevated temperatures. The major findings of the paper include:

1. Both the proposed finite element thermal and mechanical models are calibrated to be able to simulate properly the thermal and structural behviour of headed shear connectors in push-out tests either in the room temperature or under the standard fire. The proposed finite element models are also considered to be an efficient way to extend the scope of current experimental investigations into specimens of different but similar material properties and dimensional configurations.

2. Due to the relatively higher thermal conductivity of the steel material, the temperatures in shear connectors are typical 100 to 150°C higher than the surrounding concrete for a fire resistant period of 1 to 2 hrs. This leads to a faster deterioration in the shear connectors as compared with the surrounding concrete, and the failure mode may possibly switch from the crashing and splitting of the surrounding concrete as commonly understood to the yielding and over-turning of the shear connector itself.

3. Negative displacement due to major thermal expansion is observed in specimens with both solid and composite slabs. The thermal expansion behavior depends heavily on the material thermal expansion coefficient and concrete mass. It should be noted that the similar thermal expansion also exhibits in composite beams under elevated temperatures, and may be transformed into thermal stresses under various levels of longitudinal restrains.

4. Due to the relatively high temperature at the bottom layers of the concrete material, the maximum stress concentrated at a relatively high position of roughly 35 to 55 mm from the bottom of the shear connectors in push-out tests under fire. This generates a relative large over-turning moment about the bottom of the shear connector as combined with the shear load. Thus, the headed shear connectors may fail in an 'over-turning' mode instead of the well-known 'shearing-off' mode, which leads to a lower load carrying capacity and is not preferable.

Acknowledgements

References

ABAQUS (2006), *User's Manual, Version 6.4*, Hibbitt, Karlsson and Sorensen Inc.
British Standards Institution BSI (1990), *BS5950: Structural Use of Steelwork in Building, Part 3 Section 3.1:*

Code of Practice for Design of Composite Beams.

British Standards Institution BSI (2002), *Eurocode 1: Actions on Structures, Part 1.2: General Actions — Actions on Structures Exposed to Fire*, BSI, BS EN 1991-1-2.

British Standards Institution BSI (2004), *Eurocode 4: Design of Composite Steel and Concrete Structures, Part 1.1: General Rules and Rules for Buildings*, BSI, BS EN 1994-1-1.

British Standards Institution BSI (2005), *Eurocode 4: Design of Composite Steel and Concrete Structures, Part 1.2: General Rules – Structural Fire Design*, BSI, BS EN 1994-1-2.

Erdelyi, S. and Dunai, L. (2009), "Light-gauge composite floor beam with self-drilling screw shear connector: experimental study", *J. Steel Compos. Struct.*, **9**(3), 255-274.

Hegger, J. and Doinghaus, P. (2002), "High performance steel and high performance concrete in composite structures", *Proceedings of Composite Construction in Steel and Concrete IV*, Canada.

Johnson, R.P. and Oehlers, D.J. (1981), "Analysis and design for longitudinal shear in composite T-beams", *Proc. Inst. Civ. Eng.,* **71**, 989-1021.

Kim, B., Wright, H.D. and Cairn, R. (2001), "The behavior of through-deck welded shear connectors: an experimental and numerical study", *J. Constr. Steel Res.,* **57**, 1359-1380.

Lam, D. and El-Lobody, E. (2005), "Behavior of headed stud shear connectors in composite beam", *J. Struct. Eng.*, **131**(1), 96-107.

Mottram, J.T. and Johnson, R.P. (1990), "Push tests on studs welded through profiled steel sheeting", *Struct. Eng.*, **68**(10), 187-193.

Ollgaard, J.G., Slutter, R.G. and Fisher, J.W. (1971), "Shear strength of stud connectors in lightweight and normal-weigh concrete", *Am. Inst. Steel Constr. Eng. J.*, **8**(2), 55-62.

Oehlers, D.J. and Johnson, R.P. (1987), "The strength of stud shear connectors in composite beams", *Struct. Eng.*, **65**(2), 44-48.

Patrick, M. (2000), "Experimental investigation and design of longitudinal shear reinforcement in composite edge beams", *Pr. Struct. Eng. Mater.,* **2**, 196-217.

Standards Australia (1996), *Australian Standard AS2327.1. Composite Structures, Part 1: Simply Supported Beams*, Standards Australia International Ltd.

Wang, A.J. (2009), "Numerical studies of structural behaviour of shear connectors in push-out tests", *Austr. J. Struct. Eng.*, **9**(2), 79-96.

Zhao, B. and Kruppa, J. (2002a), "Experimental and numerical investigation of fire behaviour of steel and concrete composite beams", *Proceedings of Composite Construction in Steel and Concrete IV*, Canada, 129-142.

Zhao, B. and Kruppa, J. (2002b), "Simple calculation method of fire resistance of continuous composite steel and concrete beams", *Proceedings of Composite Construction in Steel and Concrete IV*, Canada, 780-792.